12

DAVID W. TAYLOR NAVAL SHIP RESEARCH AND DEVELOPMENT CENTER

Bethesda, Md. 20084

LEVEL II

RESISTANCE MEASUREMENTS OF TYPICAL PLANING BOAT APPENDAGES

by

D. Gregory and T. Beach

APPROVED FOR PUBLIC RELEASE: DISTRIBUTION UNLIMITED

SHIP PERFORMANCE DEPARTMENT

DEPARTMENTAL REPORT

DECEMBER 1979

DTNDRDC/SPD-0911-01

MAJOR DTNSRDC ORGANIZATIONAL COMPONENTS

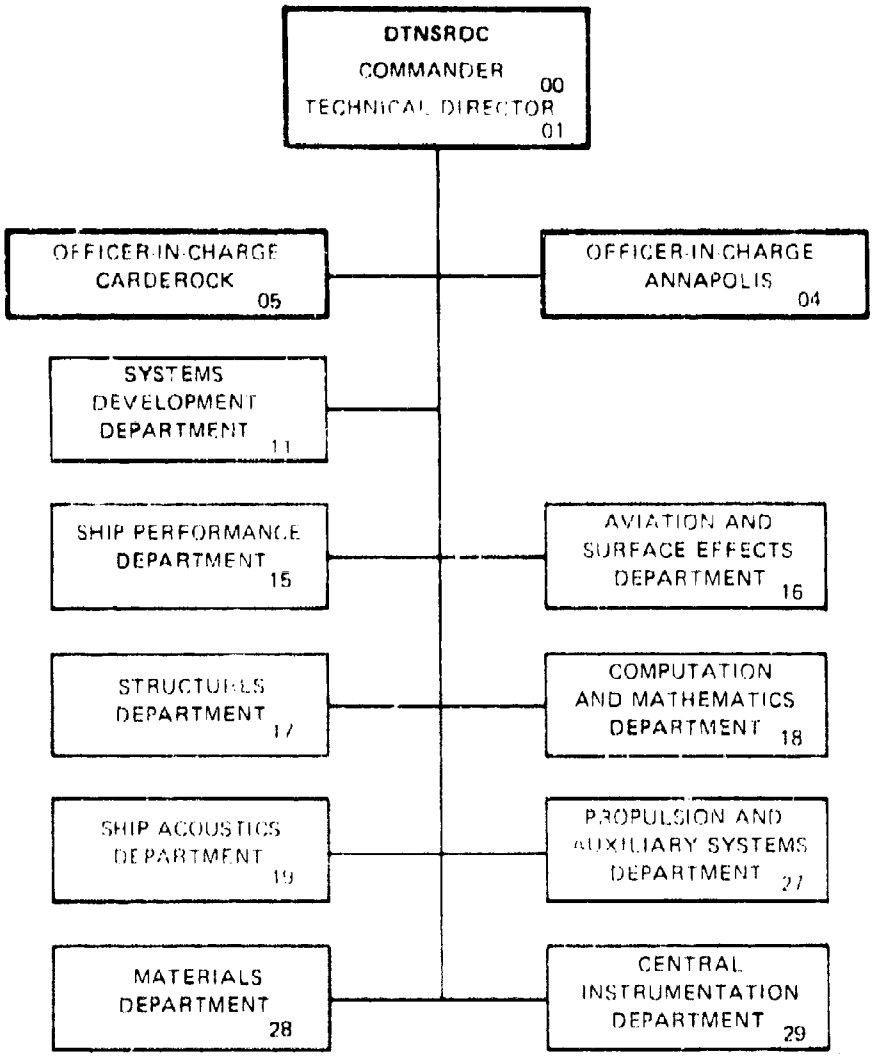

UNCLASSIFIED

SECURITY CLASSIFICATION OF THIS PAGE (When Data Entered)

REPORT DOCUMENTATION PAGE

READ INSTRUCTIONS BEFORE COMPLETING FORM

1. REPORT NUMBER: DTNSRDC/SPD-0911-01	2. GOVT ACCESSION NO.
3. RECIPIENT'S CATALOG NUMBER	
4. TITLE (and Subtitle): Resistance Measurements of Typical Planing Boat Appendages	5. TYPE OF REPORT & PERIOD COVERED: Final SPD-0911-01
	6. PERFORMING ORG. REPORT NUMBER
7. AUTHOR(s): D. Gregory [redacted] T. Beach	8. CONTRACT OR GRANT NUMBER(s)
9. PERFORMING ORGANIZATION NAME AND ADDRESS: Ship Performance Department, David W. Taylor Naval Ship R&D Center, Bethesda, Md. 20084	10. PROGRAM ELEMENT, PROJECT, TASK AREA & WORK UNIT NUMBERS: SF 43-421-001, 1-1500-103-89
11. CONTROLLING OFFICE NAME AND ADDRESS	12. REPORT DATE: Dec [redacted] 79
	13. NUMBER OF PAGES: 30
14. MONITORING AGENCY NAME & ADDRESS (if different from Controlling Office)	15. SECURITY CLASS. (of this report): APPROVED FOR PUBLIC RELEASE: DISTRIBUTION UNLIMITED
	15a. DECLASSIFICATION/DOWNGRADING SCHEDULE

16. DISTRIBUTION STATEMENT (of this Report)

Approved for Public Release: Distribution Unlimited

17. DISTRIBUTION STATEMENT (of the abstract entered in Block 20, if different from Report)

18. SUPPLEMENTARY NOTES

19. KEY WORDS (Continue on reverse side if necessary and identify by block number)

Resistance, Drag, Appendage Drag, Planing Boat Appendages

20. ABSTRACT (Continue on reverse side if necessary and identify by block number)

Full size models of typical planing boat appendages were assembled in four basic configurations. Towing basin experiments were performed to determine their drag and lift characteristics. The results are compared with predicted values derived from published empirical formulas. Experimental drag is found to be higher than the predictions, and the lift displays a speed dependence that is not considered by the existing prediction method.

DD FORM 1 JAN 73 1473 EDITION OF 1 NOV 65 IS OBSOLETE
S/N 0102-LF-014-6601

UNCLASSIFIED
SECURITY CLASSIFICATION OF THIS PAGE (When Data Entered)

TABLE OF CONTENTS

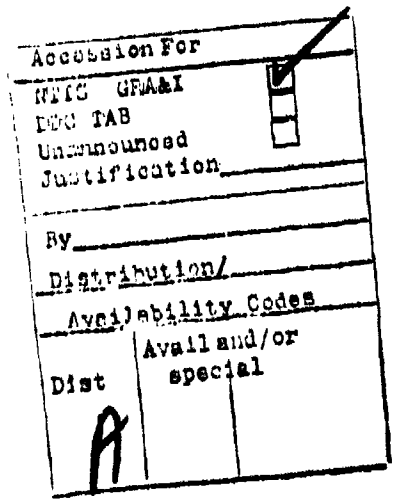

LIST OF FIGURES

LIST OF TABLES

NOMENCLATURE

		Dimensions*
A_o	Propeller disk area = $\pi D_p^2/4$	L^2
C_{DP}	Appendage drag coefficient based on propeller disk area	-
C_{DR}	Rudder drag coefficient based on rudder planform area	-
C_{LP}	Appendage lift coefficient based on propeller disk area	-
C_f	Schoenherr line friction drag coefficient	-
D	Drag force, general	MT^2L^{-1}
D_A	Appendage drag force	MT^2L^{-1}
D_p	Propeller diameter	L
D_{TOTAL}	Total measured drag force, appendages plus friction plate	MT^2L^{-1}
D_{PLATE}	Measured drag force on friction plate alone	MT^2L^{-1}
d	Diameter of shaft or barrel	L
L	Lift force, general	
L_{TOTAL}	Total measured lift force, appendages plus friction plate	MT^2L^{-1}
L_{PLATE}	Measured lift force on friction plate alone	MT^2L^{-1}
ℓ	Length of shaft or barrel	L
m	Slope of drag force versus V_K^2, general	MT^4L^{-3}

*L = length, T = time, M = mass

		Dimensions
m_A	Slope of appendage drag force versus V_K^2; may be specified for complete appendage set, forward appendages (without rudder), or for the rudder alone	MT^4L^{-3}
R_{nd}	Reynolds number based on shaft or barrel diameter = Vd/ν	-
$R_{n\ell}$	Reynolds number based on shaft or barrel length = $V\ell/\nu$	-
R_{nc}	Reynolds number based on strut chord	-
S	Planform area of strut	L^2
t/c	Thickness-to-chord ratio of strut	-
V	Speed	LT^{-1}
V_K	Speed in knots	LT^{-1}
ε	Shaft angle	degrees
ν	Kinematic viscosity of water	L^2T^{-1}
ρ	Mass density of water	ML^{-3}

ABSTRACT

Full size models of typical planing boat appendages were assembled in four basic configurations. Towing basin experiments were performed to determine their drag and lift characteristics. The results are compared with predicted values derived from published empirical formulas. Experimental drag is found to be higher than the predictions, and the lift displays a speed dependence that is not considered by the existing prediction method.

ADMINISTRATIVE INFORMATION

This work was authorized by the Naval Material Command (08T23), and funded under the Ship Performance and Hydromechanics Task Area SF 43-421-001, work unit 1-1500-103-89, administered by the Ship Performance Department of the David W. Taylor Naval Ship Research and Development Center.

INTRODUCTION

Drag forces on the appendages of a planing craft can be as much as twenty-five percent of the total craft drag. Traditionally, these forces have been predicted by using empirical equations or by subscale model data. In order to alleviate the uncertainties in the prediction scheme and in Reynolds scaling of appendage forces, experiments were performed in the Carriage 5 towing basin of the David W. Taylor Naval Ship Research and Development Center on full size models typical of current Navy designs. These full size appendages are representative of those for a typical 35 foot, twin screw planing craft, propelled by 20-inch diameter propellers.

MODEL DESCRIPTION

Four appendage configurations were tested, each consisting of a propeller shaft, a strut barrel, a strut, and a rudder. Side views of the arrangements with propeller shaft angles of 7.5, 10, and 15 degrees are shown in Figures 1 through 3, respectively. A single strut was used at all three angles. The V-strut configuration (see Figure 4) was tested at the 10 degree shaft angle only. The propeller shafts were 1.5 inches (3.81 cm) in diameter, and the barrels were 4.5 inches (11.43 cm) in

References are listed on page 9.

diameter. Struts were machined with a cross section shown in Figure 5. The rudder was a flat plate, 0.5 inch (1.27 cm) thick, with a rounded leading edge. The models were mounted on an aluminum friction plate, whose planform is shown in Figure 6. Figure 7 is a photograph of the single strut configuration, with the 10° shaft, ready to be placed in the basin for testing. The surface finish and fairing of these full size appendages was made representative of typical current manufacturing practices.

EXPERIMENTAL PROCEDURE

The friction plate was mounted at two points, as seen in Figure 7, to a dynamometer consisting of a system of modular force gauges for measuring drag and lift independently as forces horizontal and perpendicular to the friction plate. The dynamometer was bolted to struts which were mounted to the heavy bridge of Carriage 5. Data were taken with the friction plate submerged to a depth of 3 feet (0.91 m) below the free surface. This appeared to be satisfactory for preventing any ventilation of the appendage configurations mounted on the underside of the plate. Water temperature remained constant during the experiments at $71^{\circ}F$ ($22^{\circ}C$), so the water mass density and kinematic viscosity were taken as $\rho = 1.936$ slugs/feet^3 (997.8 kg/m^3) and $\nu = 1.0414 \times 10^{-5}$ feet^2/second (9.674×10^{-7} m^2/s), respectively.

Error estimates have been determined based on the calibrated performance of the assembled dynamometer and the known accuracy performance of the block gauges. The expected range of error for the drag measurement is about 1.5 percent of the total measured value. This translates to absolute error values in drag of about ± 2 to ± 15 pounds (6.68 to 66.8 N) across the speed range, with corresponding total drag forces varying from 100 to 1000 pounds (445 to 4450 N). The accuracy of the lift force measurements is somewhat worse than that of the drag, especially at the lower speeds, due to small lift values, and because the net lift value represents small differences of large measured forces at the fore and aft lift gauges. Lift force errors range from ± 5 to ± 20 pounds (22.3 to 89 N) across the entire speed range.

EXPERIMENTAL RESULTS

DRAG DATA

Measured drag data are shown graphically as the variation of drag force with speed squared in Figures 8 through 12. All these curves are linear in V_K^2, and this affords very simple, yet universal characterizations of the appendage drag, both in dimensional and nondimensional terms.

First, in dimensional terms, the drag force can be fitted by the general expression

$$D = mV_K^2 \tag{1}$$

where D = measured drag force, pounds(Newtons)
m = constant slope, pounds/knot^2 (Newtons/knot^2)
V_K = forward speed, knots

For each configuration, the slope of the best faired line through the data was determined, with a maximum deviation of ± 2 percent. The net appendage drag is taken as the difference between the total measured drag and the drag of the friction plate alone. Then the net appendage drag force

$$D_A = D_{TOTAL} - D_{PLATE} \tag{2}$$

can be expressed as

$$D_A = m_A V_K^2 \tag{3}$$

where m_A = constant slope of the net appendage drag force, pounds/knot^2 (Newtons/knot^2)

In nondimensional terms, the appendage drag coefficient is defined as

$$C_{DP} = \frac{D_A}{\frac{1}{2}\rho V^2 A_o} \tag{4}$$

where ρ = mass density of water
V = forward speed
A_o = propeller disk area = $\pi D_p^2/4$

The area used in forming nondimensional drag coefficients is the disk area of a typically sized propeller that would correspond to the sizes of these appendages. In this case

$$D_p = 20 \text{ inches } (0.51 \text{ m})$$

so that

$$A_o = 2.182 \text{ feet}^2 \ (0.2043 \text{ m}^2)$$

It may be assumed that the actual wetted surface of the appendages is directly proportional to the propeller disk area, since the sizes of the appendage components are principally functions of the size of the propeller. Thus, the present appendage drag coefficients are in a form directly useful in the design process.

The experimental values for the appendage drag slopes, m_A, as well as the appendage drag coefficients, C_{DP}, are given in Table 1 for the several configurations tested. Note that separate results are shown for the drag on the forward appendages (appendage set without the rudder) as well as for the complete set. Also included is the usual rudder-alone drag coefficient based on the rudder planform area.

It is of interest to note that the drag of the V-struts is not significantly different from that of a single strut. The difference is less than five percent for the same shaft angle and strut element thickness-to-chord ratio. This difference would represent less than two percent difference in total craft drag. The small drag penalty due to the V-strut is outweighed by its structural benefits in comparison with the single strut arrangement.

It may also be observed that the sum of the rudder drag and the drag of the forward appendages, tested separately, is on the order of 15 percent higher than the drag measured for the combination. This difference is due to the fact that for the combined configurations, the rudder was operating in the wake of the forward appendages, so that the net inflow velocity was less than the free stream velocity. It follows that the effect of the wake on the rudder drag for the V-strut configuration should be less pronounced. As seen from the data, this indeed is the case.

LIFT DATA

Measured lift performance is shown graphically as the variation of lift force with speed squared in Figures 13 through 17. These data are for the total measured lift on the forward appendages (without rudder) plus friction plate, with the results of the friction plate alone shown in Figure 13. Smooth curves were drawn through the data and the faired values were used in calculating net appendage lift coefficients.

The nondimensional lift coefficient for net appendage lift without rudder is defined as

$$C_{LP} = \frac{L_{TOTAL} - L_{PLATE}}{\frac{1}{2}\rho V^2 A_o} \qquad (5)$$

where L_{TOTAL} = lift of the appendages plus the friction plate

L_{PLATE} = lift of the friction plate alone

Lift coefficients for the various forward appendage configurations are plotted as a function of speed in Figure 18. As seen in the figure, relatively larger lift coefficients are evident below 20 knots. Practically zero appendage lift was generated above 20 knots. At the low speed end of these experiments ($V_K \leq 20$ knots) there is evidently a slight but consistent increase in the appendage lift coefficient as the shaft angle is increased from 7.5 degrees to 15 degrees, and a further slight increase in going to the V-strut supported shaft at 10 degrees.

DATA COMPARISON WITH PREDICTION

The method described in Reference 1 can be used for predicting the drag and lift forces on arrangements of inclined-shaft appendage sets. For reference, the empirically-based equations quoted by Hadler[1] are repeated here for each of the appendage components.

Shaft and Barrel (defined for $R_{nd} \leq 5.5 \times 10^5$)

$$D = \frac{1}{2} \rho \ell d V^2 (1.1 \sin^3 \varepsilon + \pi C_f) \tag{6}$$

$$L = \frac{1}{2} \rho \ell d V^2 (1.1 \sin^2 \varepsilon \cos \varepsilon) \tag{7}$$

where

ℓ = length of shaft or barrel
d = diameter of shaft or barrel
ε = shaft angle
ρ = mass density of water
V = speed
C_f = Schoenherr friction coefficient based on R_{nd}

Strut and Rudder

$$D = \frac{1}{2} \rho S V^2 [2C_f (1+2(t/c) + 60(t/c)^4)] \tag{8}$$

where

S = planform area of strut or rudder
t/c = thickness-to-chord ratio
C_f = Schoenherr friction coefficient based on R_{nc}

For purposes of comparison, these prediction equations have been used to estimate the drag and lift for the particular case of a 10 degree shaft angle, single strut arrangement with the same dimensions as the model used in the present experiments. The appropriate dimensions are listed below

Shaft	ℓ = 71 inches (1.8 m)
	d = 1.5 inches (3.81 cm)
	ϵ = 10 degrees
Strut Barrel	ℓ = 23 inches (0.58 m)
	d = 4.5 inches (11.4 cm)
	ϵ = 10 degrees
Strut	S = 0.71 feet^2 (0.066 m^2)
	t/c = 0.14
	c = 8 inches (20.3 cm)

The applicability of the prediction formulas is limited by the diameter Reynolds number $R_{nd} < 5.5 \times 10^5$. This narrows the range of certain validity to $V_K < 9$ knots for the strut barrel and $V_K < 27$ knots for the shaft.

Numerical values for the drag force obtained from the estimating formulas over the entire speed range of interest are given in Table 2, along with the experimental values. The comparison is shown graphically in Figure 19.

For the lift performance, the formulas predict a constant value of the lift coefficient for the inclined shaft plus barrel

$$C_{LP} = 0.0218$$

This constant value is indicated by the dashed line in the plot of measured values shown in Figure 20.

It appears that the measured drag forces are about 2.5 times as large as the predicted values. At the same time, the measured lift coefficients seem to tend toward the constant predicted value at the low end of the

experimental speed range (V_K <10 knots).

The results of the prediction formulas of Reference 1 have previously been compared with some subscale model data in Table 10 of Appendix 1 of that reference. The model data employed in this comparison were obtained by Clement[2] for planing boat appendages similar to those of the present experiments. Ratios of measured-to-predicted values of appendage drag vary from 1.45 for the 1/10-scale model to 0.97 for the 1/2-scale model. The non-uniformity of this ratio with respect to scale seems to indicate that some crucial scaling property is not being properly accounted for in the estimating formulas.

There are several differences between the model experiments of Reference 2 and the full size appendage experiments reported here. Clement's subscale models were smooth-finished, while the finish on the present full size appendages was made rougher and typical of usual boat building practice. Clement's subscale models featured strut and shaft palms, that together contributed over 30 percent of the total appendage drag for the case of 1/2-scale. No palms were used in the present full size models. It is possible that, for much of the speed range reported on in Reference 2, substantial laminar flow existed over the components of the small, smooth appendage models. The present full size appendage forces were obtained with predominantly turbulent boundary layer flows.

It appears from the present data that the prediction formulas of Reference 1 result in optimistic (too low) estimates of full scale appendage drag force. Although the predictions were carried out for speeds beyond the valid Reynolds number limit (representing 27 knots for the shaft and 9 knots for the bossing), the large discrepancy between measured and estimated drag values persists down through the low speed range as well.

It is interesting to make a separate comparison between the results of the present rudder-alone tests, previous rudder experiments, and estimates from the prediction formulas. Rudder forces were measured on subscale models in Reference 3. The configuration of one of the rudders is a reasonable approximation of a 1/3-scale version of the present full scale rudder. The subscale model had a geometric aspect ratio of 1.5 compared with the present rudder aspect ratio of 1.77. The thickness-to-chord ratio of the full size rudder is 10 percent larger than that of the

subscale model, and the diameter of the full scale rudder stock is proportionally 50 percent larger than that of the subscale model. The gap between the mounting plate and the top edge of the rudder was proportionally smaller on the subscale model than for the full size arrangement. It is difficult to predict the combined effects of these differences, but evidently the net result is higher drag. The drag coefficient for the present full size rudder based on planform area is $C_{DR} = 0.06$, compared with $C_{DR} = 0.04$ for the similar rudder tested in Reference 3. By contrast, the rudder drag coefficient predicted using the method outlined in Reference 1 is $C_{DR} = 0.008$.

For appendages of similar proportions to those reported on here, it is recommended to use the present full size drag results.

The constant lift coefficient predicted by the method of Reference 1 was not realized in the tests of the full size appendages. Present data indicate that the lift coefficients for these appendages diminish with speed and can be assumed to be zero at higher speeds (above 20 knots).

CONCLUSIONS

The information in this report is intended to be an initial data base for use in the prediction of the forces on planing craft appendages. The data presented can be used in predicting the powering requirements of planing boats up to about thirty-three knots. Extrapolation beyond this point has a degree of uncertainty due to the probable inception of cavitation. Cavitation would increase the appendage forces above the values reported here.

REFERENCES

1. Hadler, J.B., "The Prediction of Power Performance on Planing Craft," The Society of Naval Architects and Marine Engineers Transactions, Vol. 74, 1966, pp 563-600.
2. Clement, E.P., "Scale Effect on the Drag of a Typical Set of Planing Boat Appendages," DTMB Report 1165, August 1957.
3. Mathis, P.B., and P.L. Gregory, "Propeller Slipstream Performance of Four High Speed Rudders Under Cavitation Conditions," DTNSRDC Ship Performance Department Report SPD-4361, May 1974.

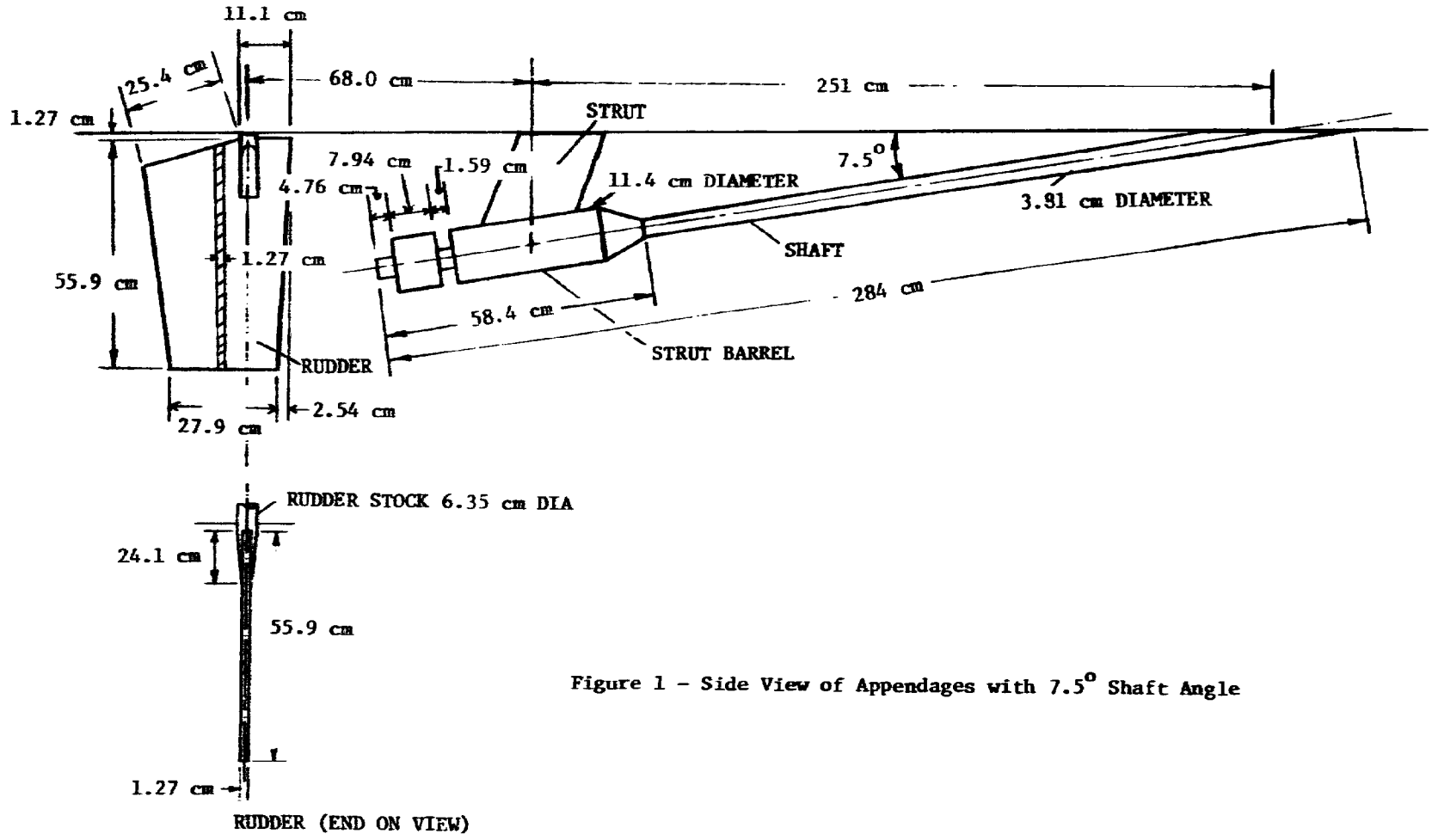

Figure 1 - Side View of Appendages with 7.5° Shaft Angle

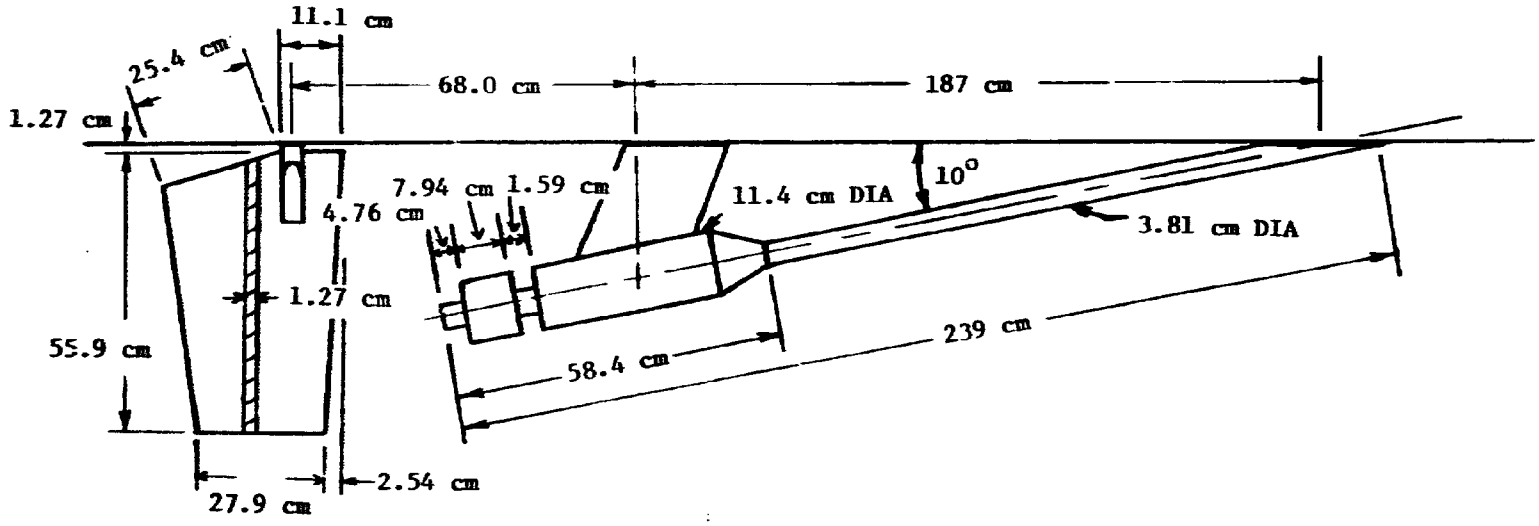

Figure 2 - Side View of Appendages with a 10° Shaft Angle

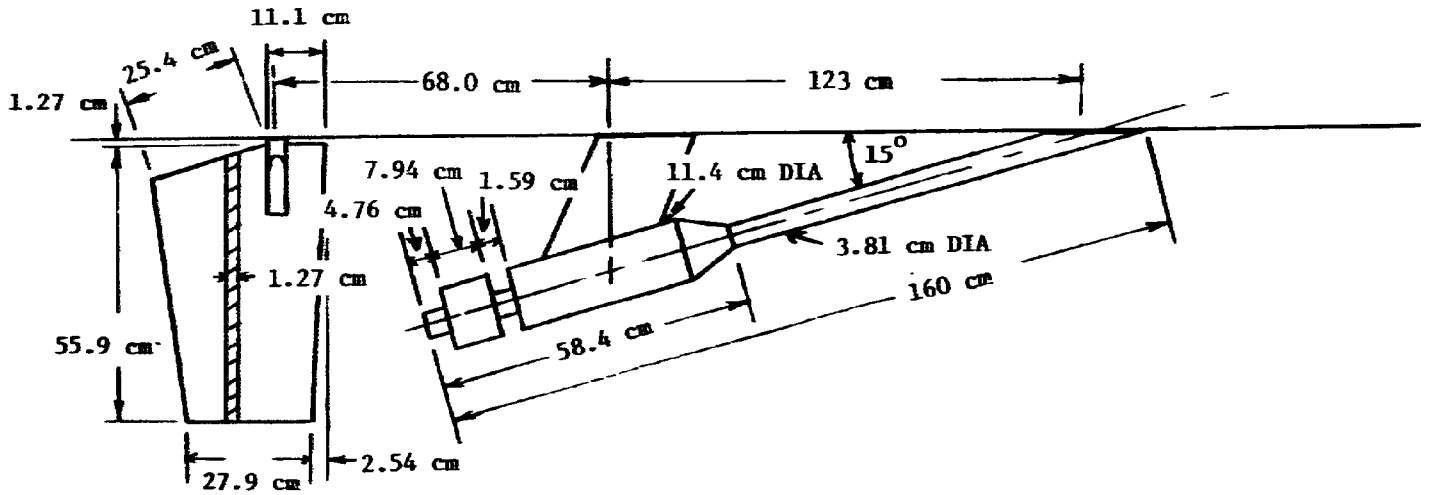

Figure 3 - Side View of Appendages with a 15° Shaft Angle

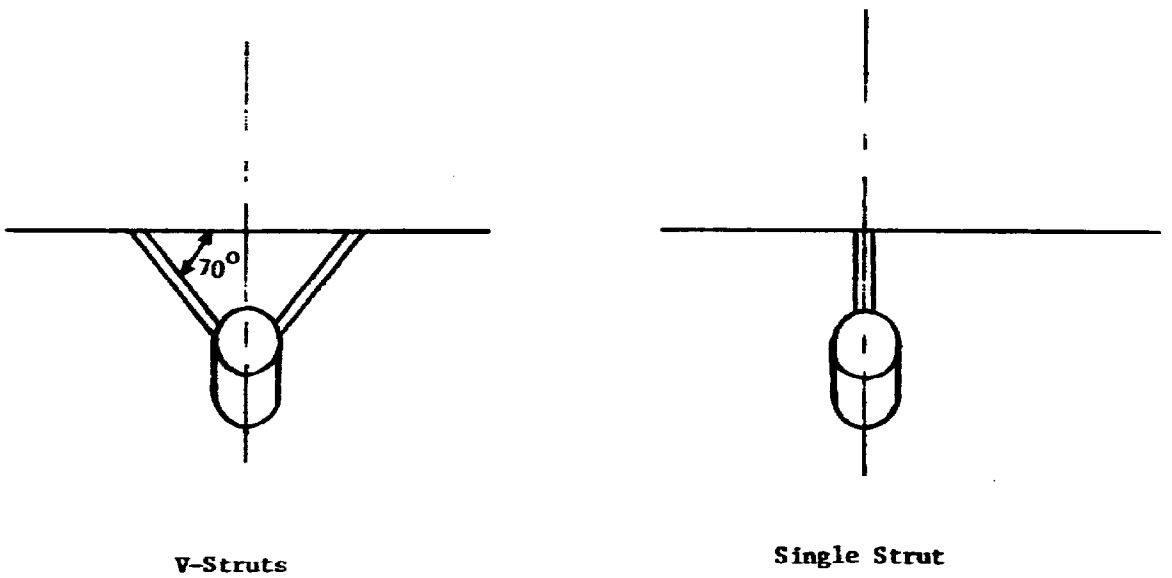

Figure 4 – Front View of Struts and Strut Barrel

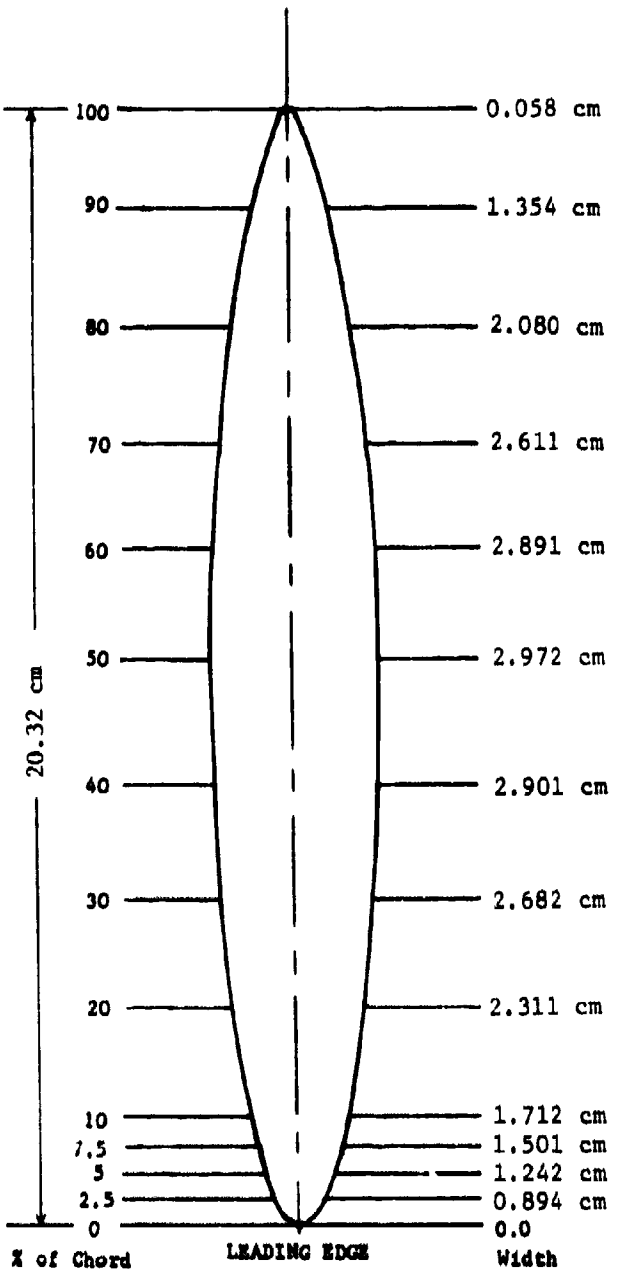

Figure 5 - NACA 16-014.63 Strut Cross Section

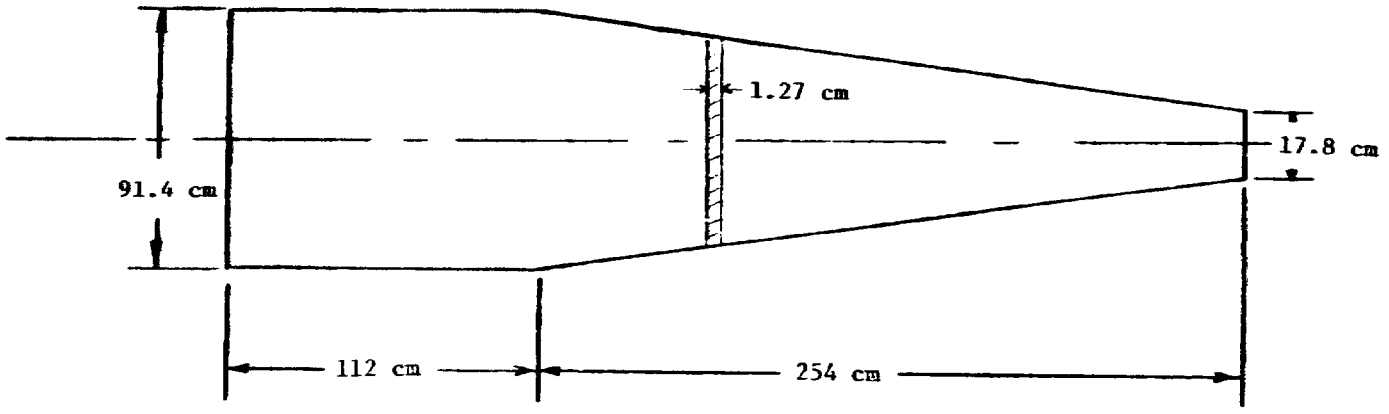

Figure 6 - Plan View of the Friction Plate

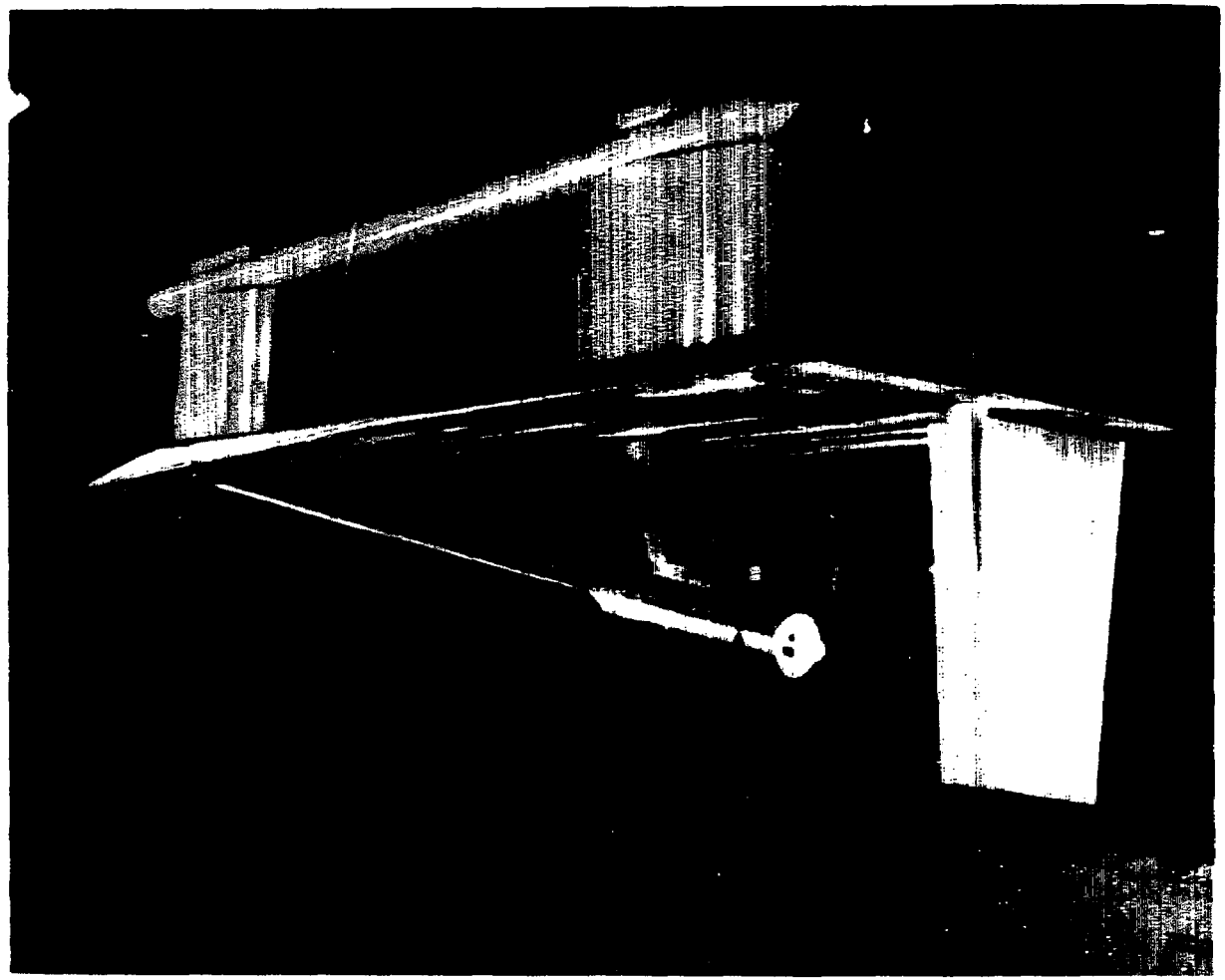

Figure 7 - Photograph of Complete Appendage Set with 10^{o} Shaft, Single Strut; Ready to be Tested

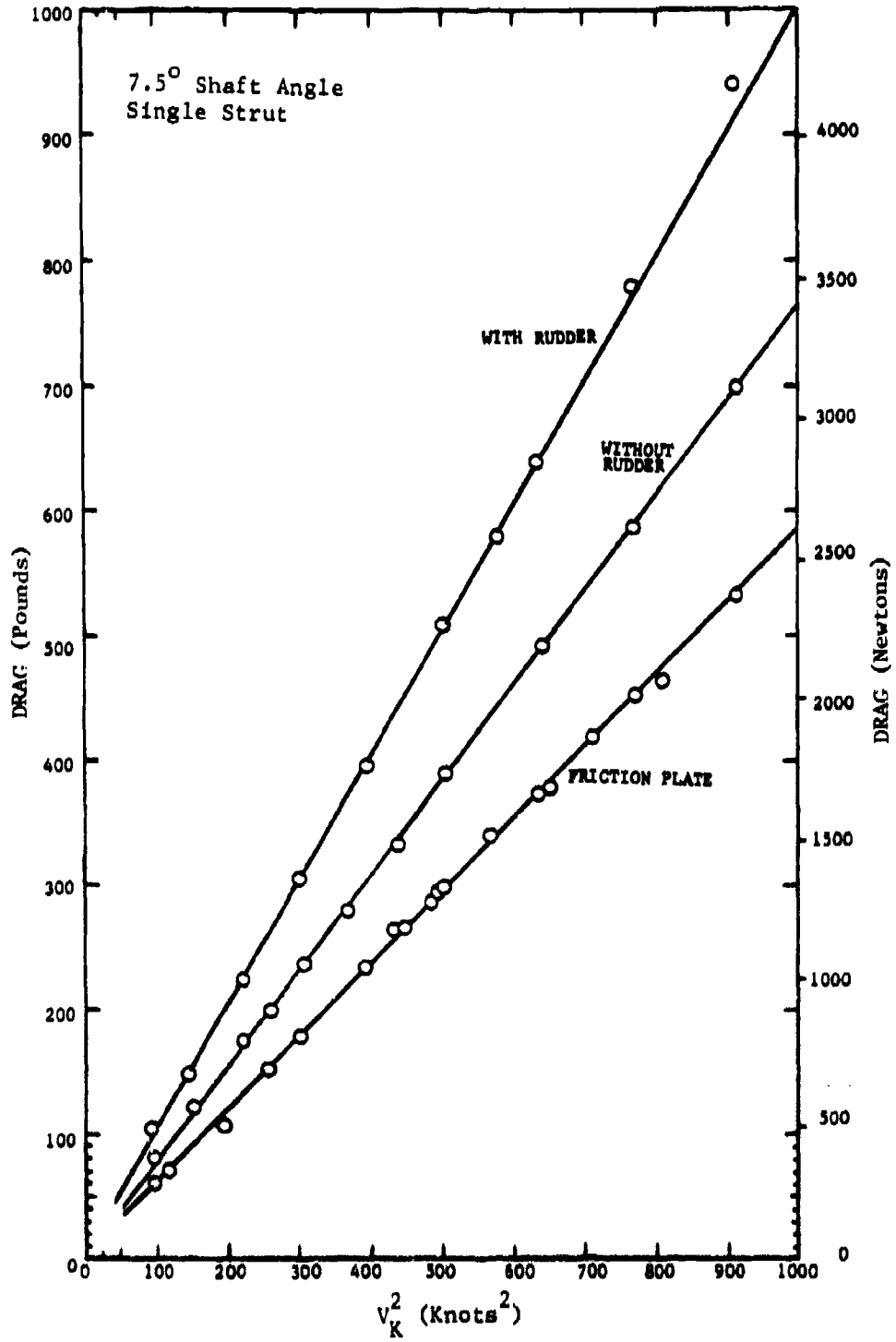

Figure 8 - Variation of Drag Force with Speed Squared for the 7.5° Shaft Appendage Configuration

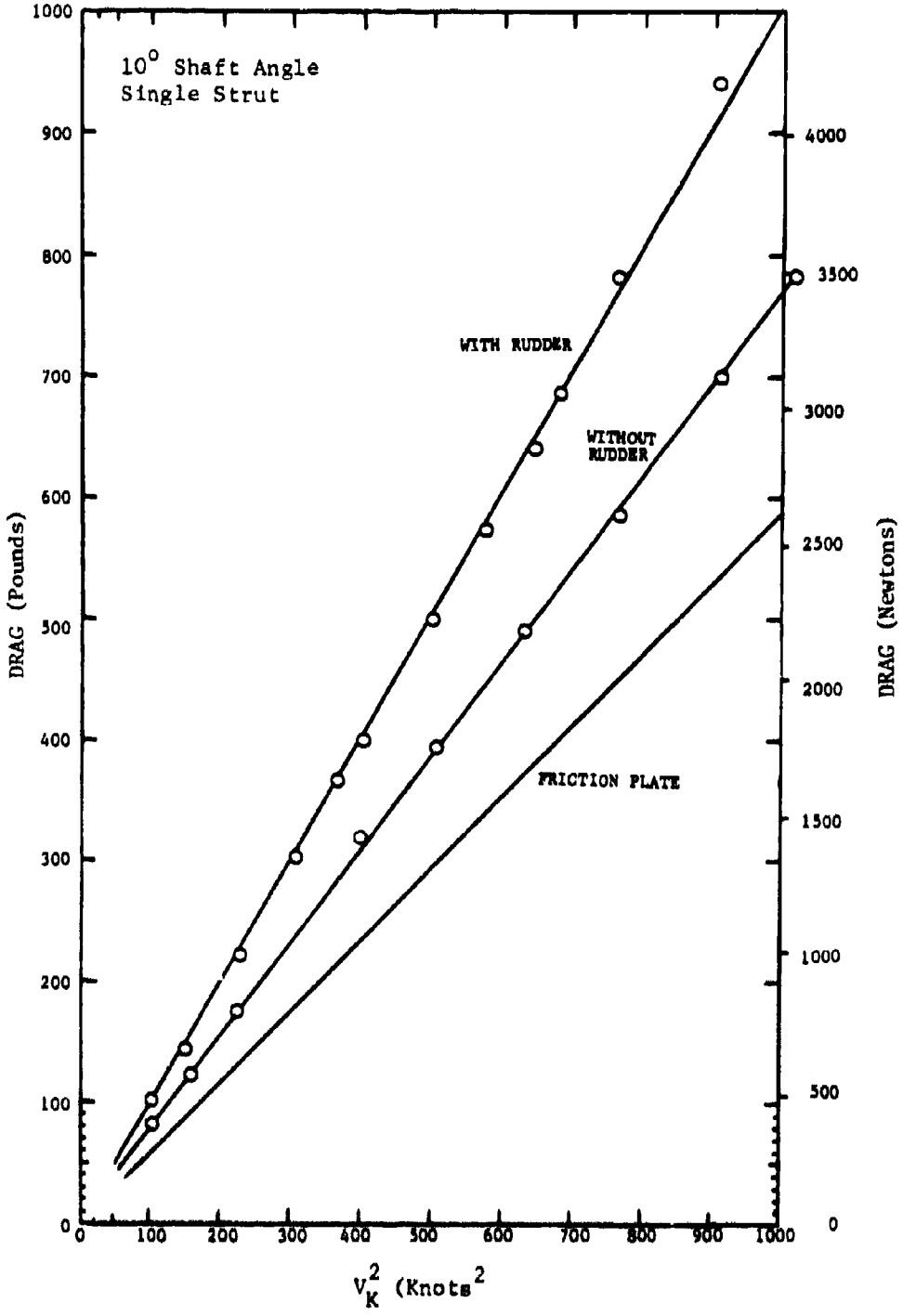

Figure 9 - Variation of Drag Force with Speed Squared for the 10° Shaft Appendage Configuration

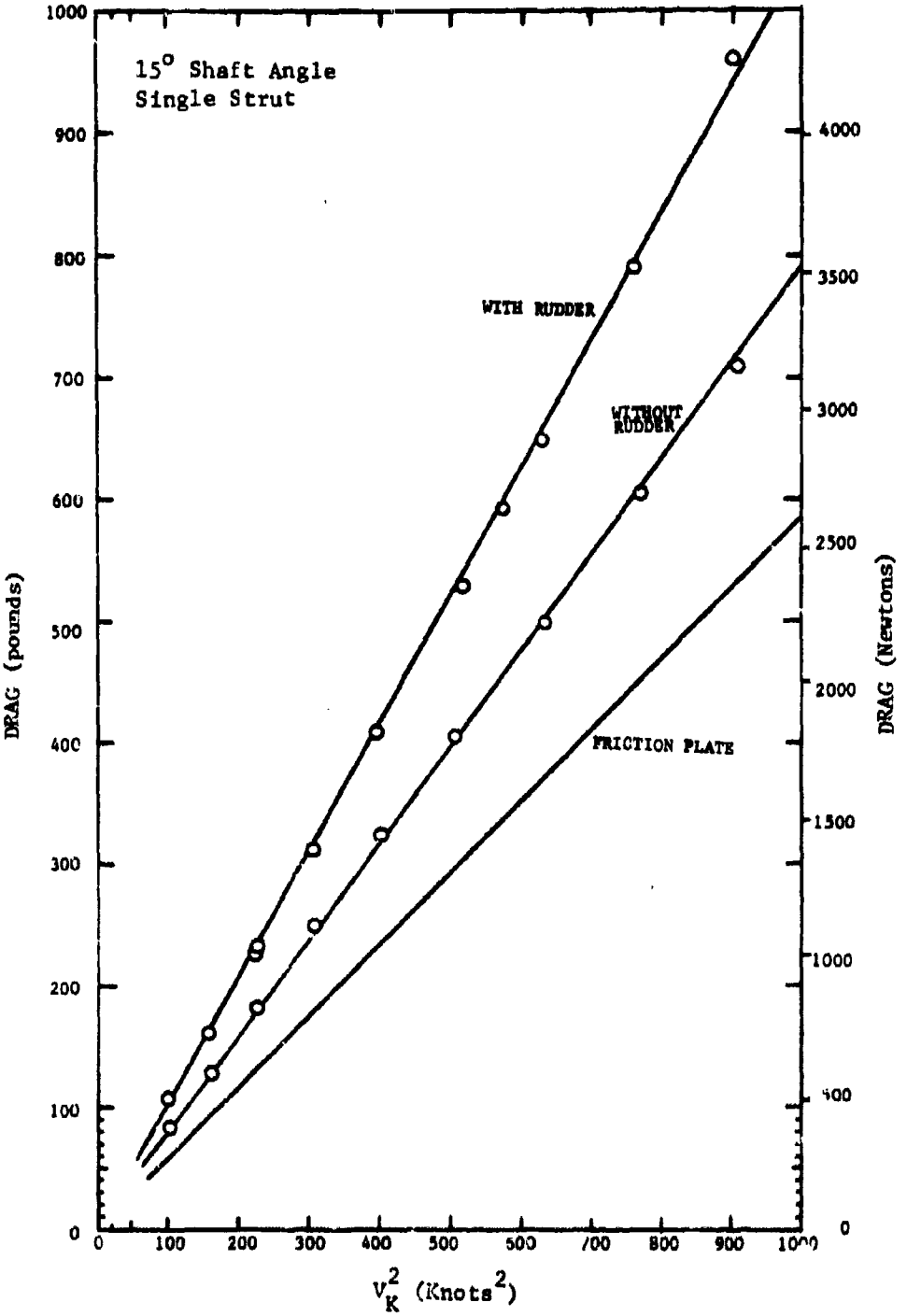

Figure 10 - Variation of Drag Force with Speed Squared for the 15° Shaft Appendage Configuration

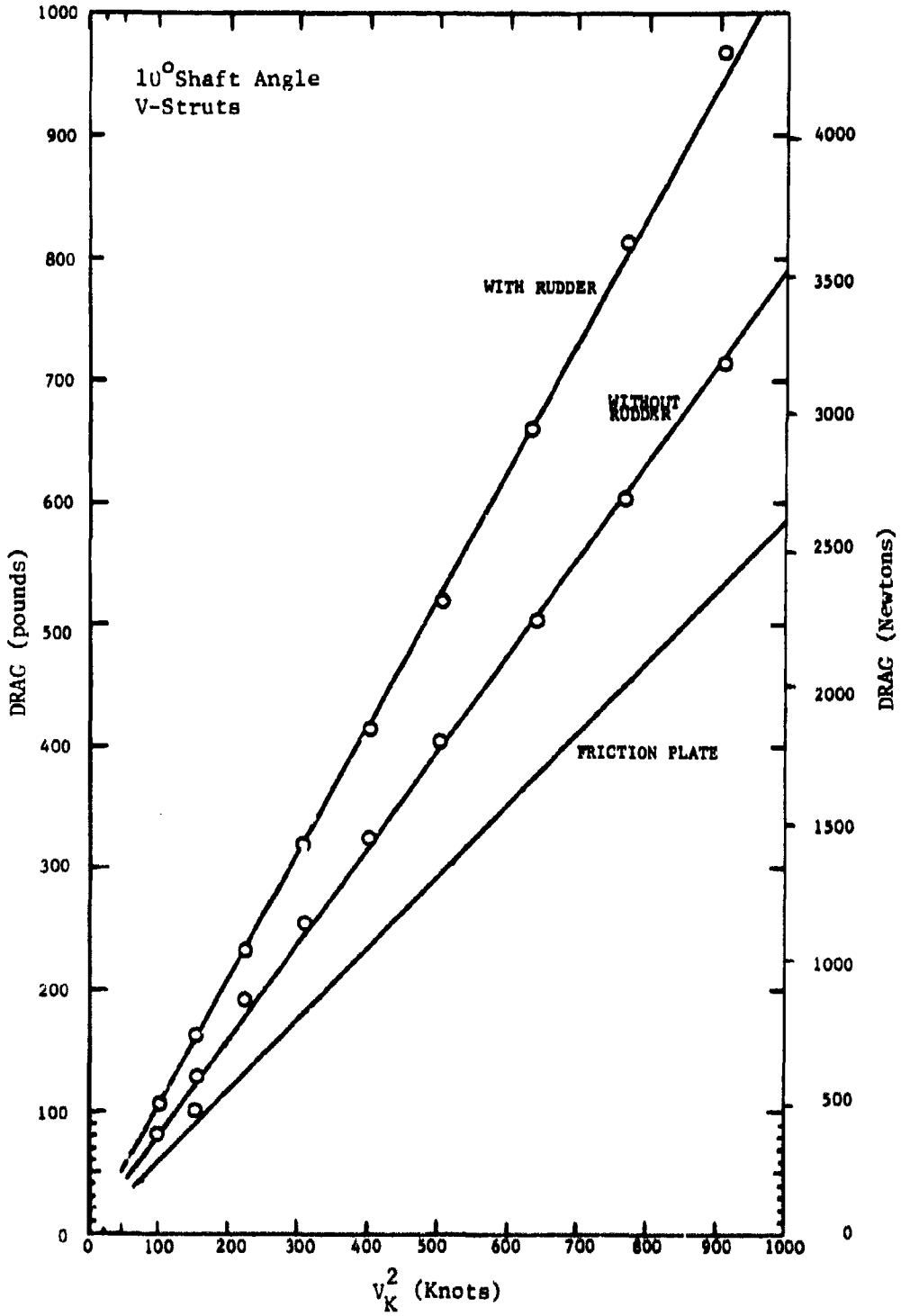

Figure 11 - Variation of Drag Force with Speed Squared for the 10° Shaft with V-Struts Appendage Configuration

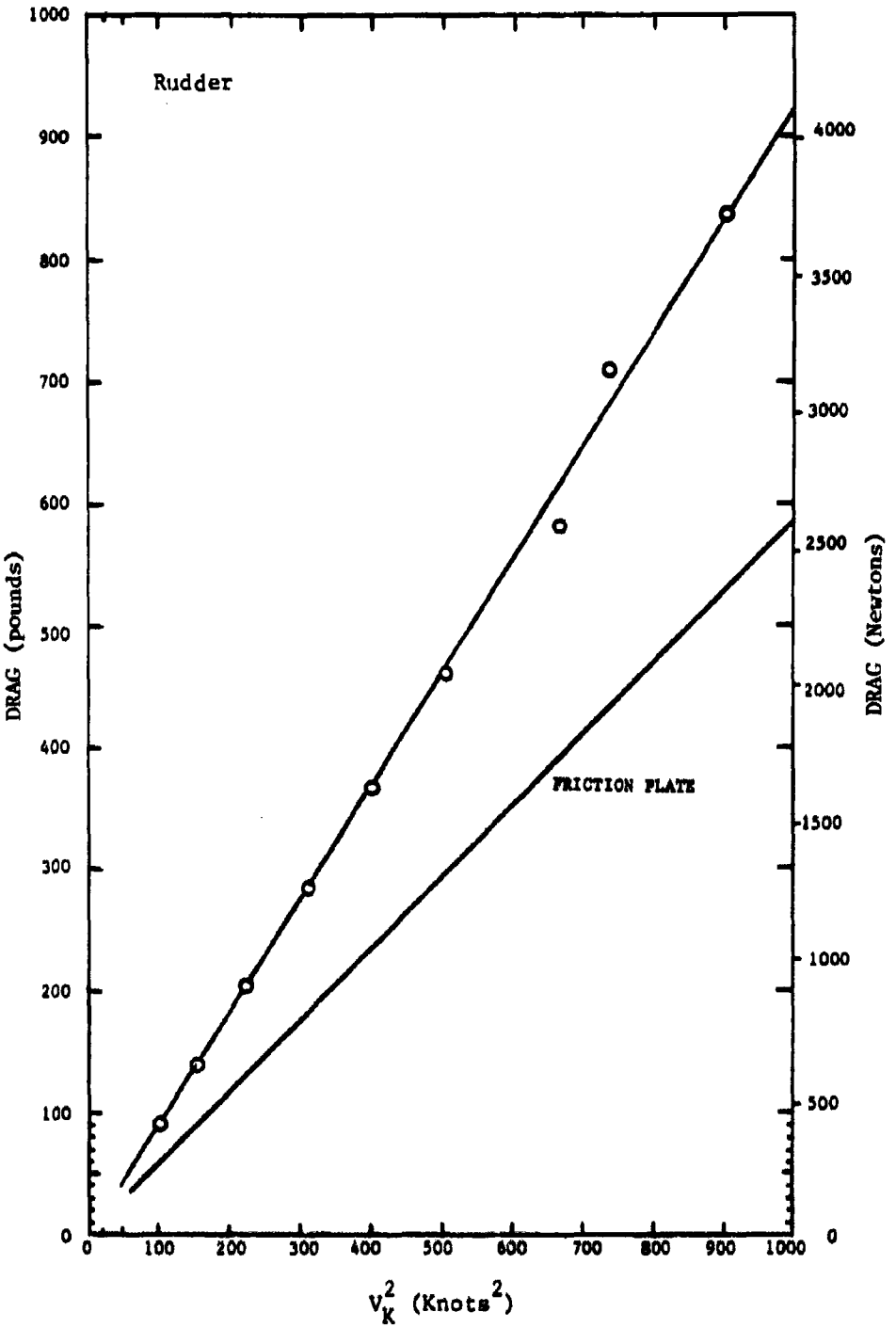

Figure 12 - Variation of Drag Force with Speed Squared for the Rudder Only

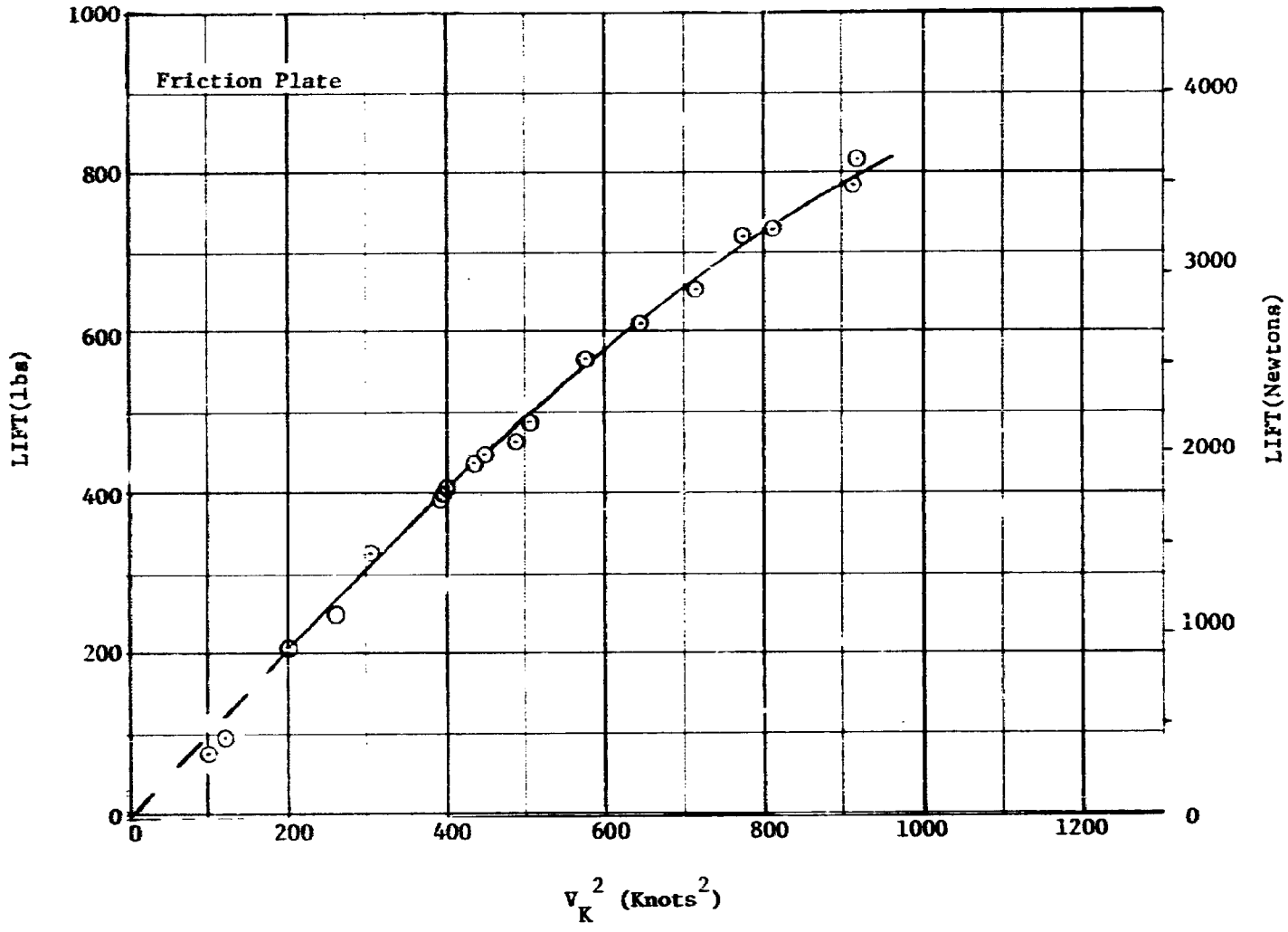

Figure 13 - Total Measured Lift Force versus Speed Squared for the Friction Plate Alone

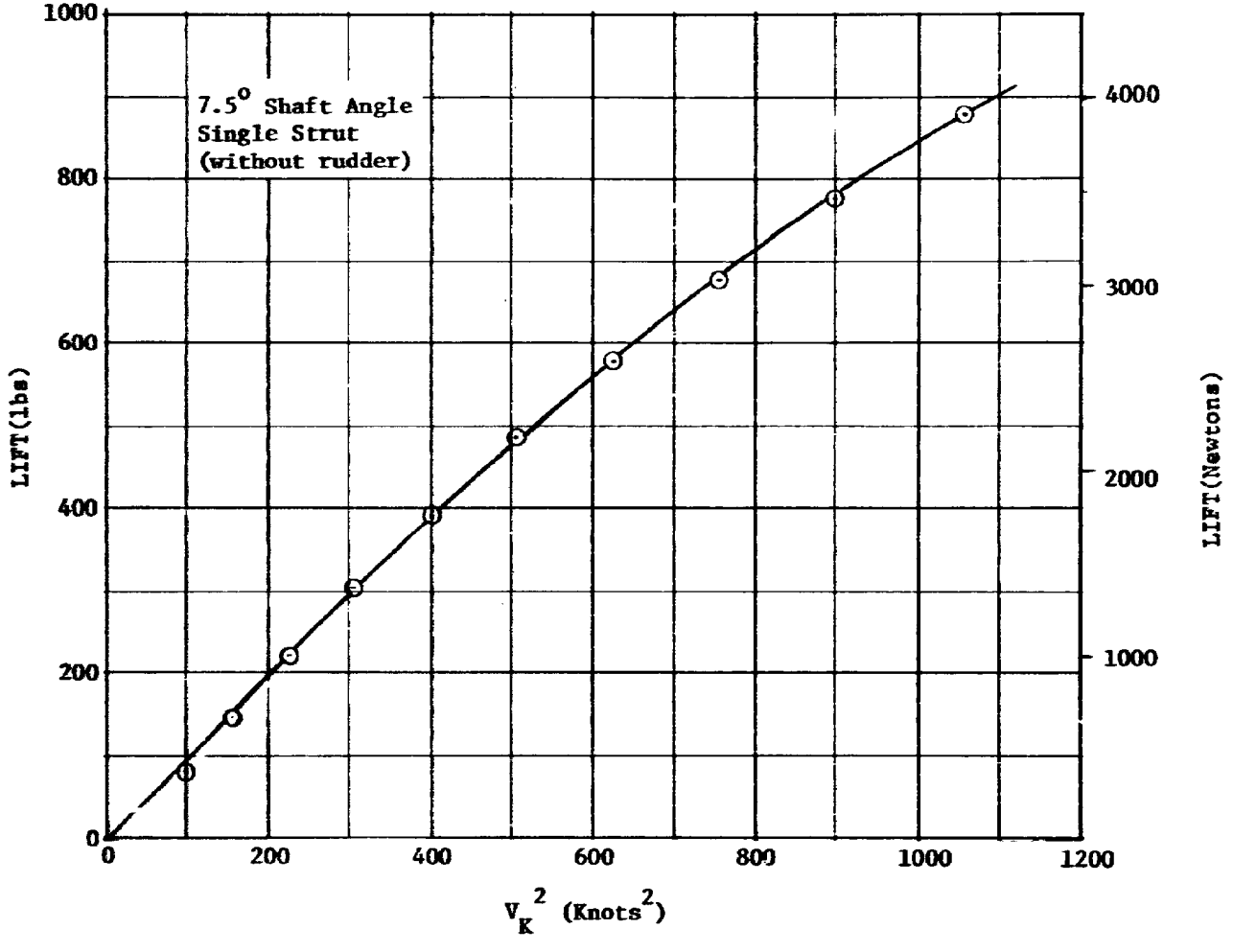

Figure 14 – Total Measured Lift Force versus Speed Squared for the Plate Plus 7.5° Shaft Forward Appendages

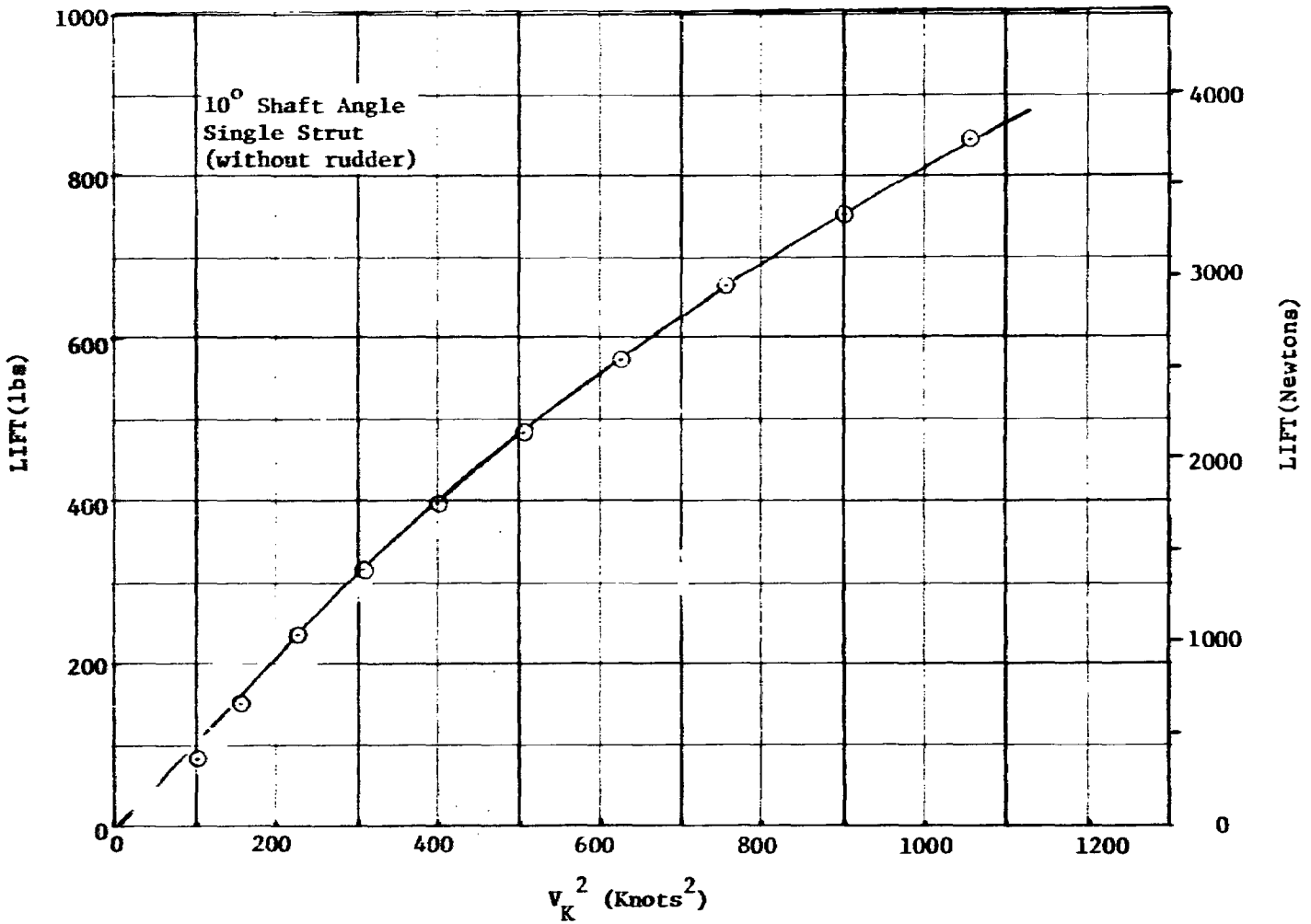

Figure 15 - Total Measured Lift Force versus Speed Squared for the Plate Plus 10° Shaft Forward Appendages

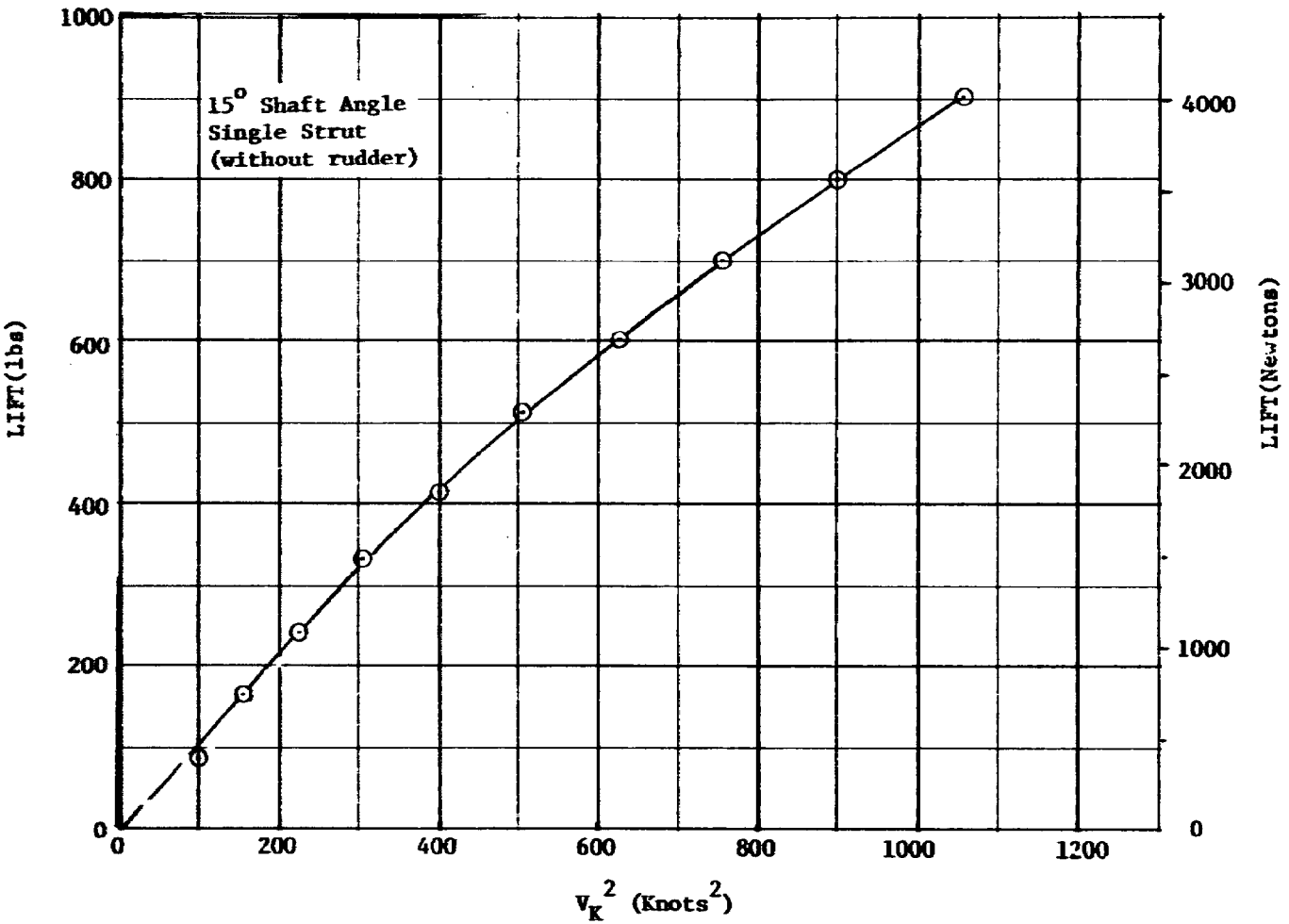

Figure 16 – Total Measured Lift Force versus Speed Squared for the Plate Plus 15° Shaft Forward Appendages

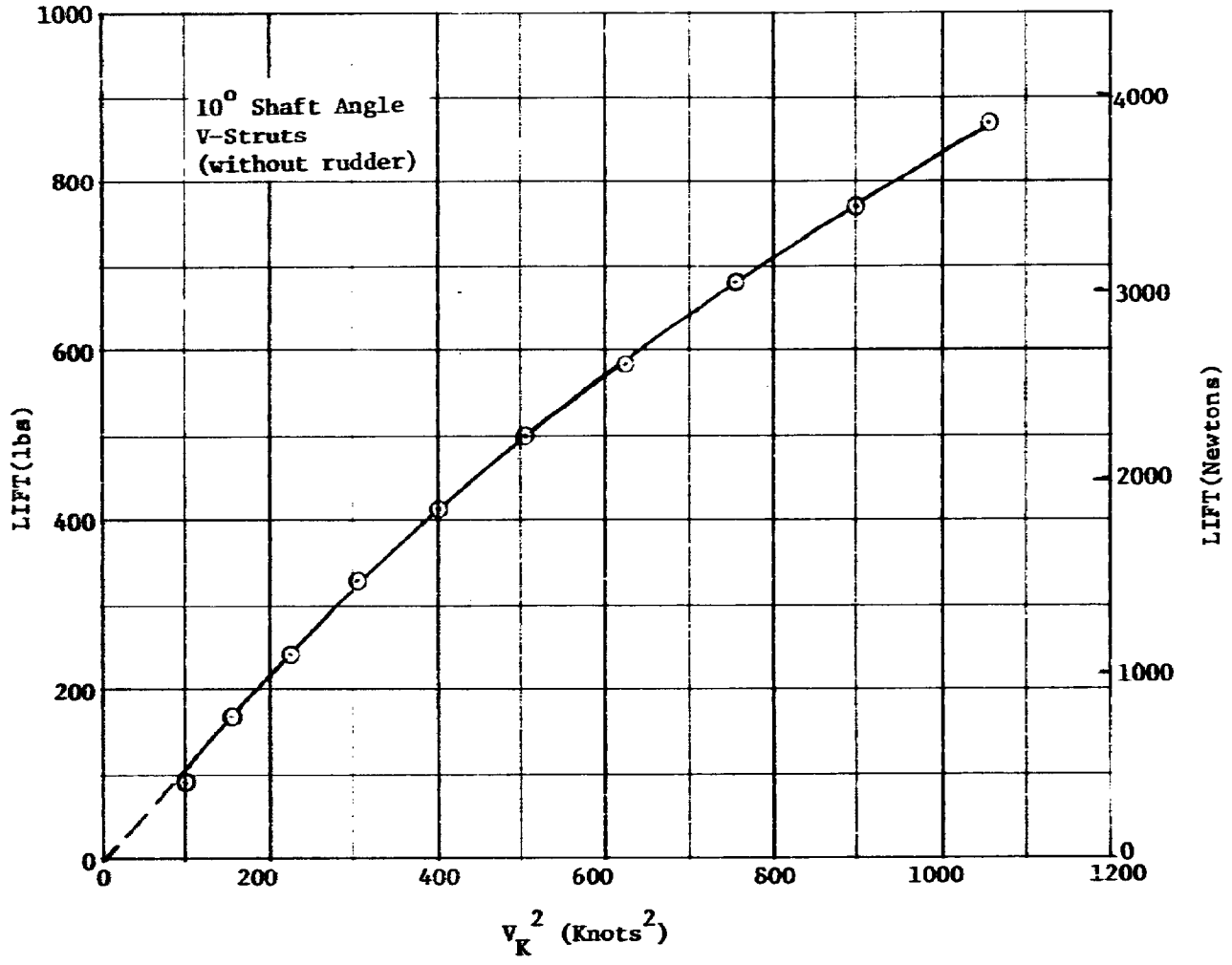

Figure 17 - Total Measured Lift Force versus Speed Squared for the Plate Plus 10° Shaft Forward Appendages with V-Struts

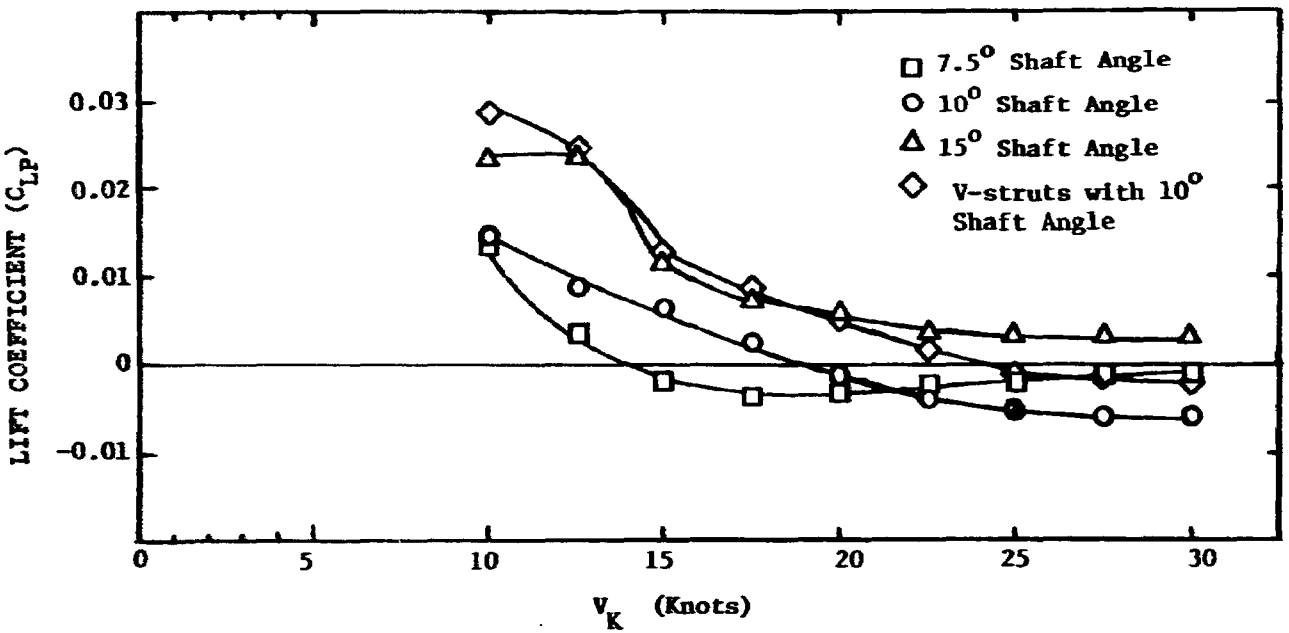

Figure 18 – Variation of Net Appendage Lift Coefficient with Speed for Each Configuration Without Rudder

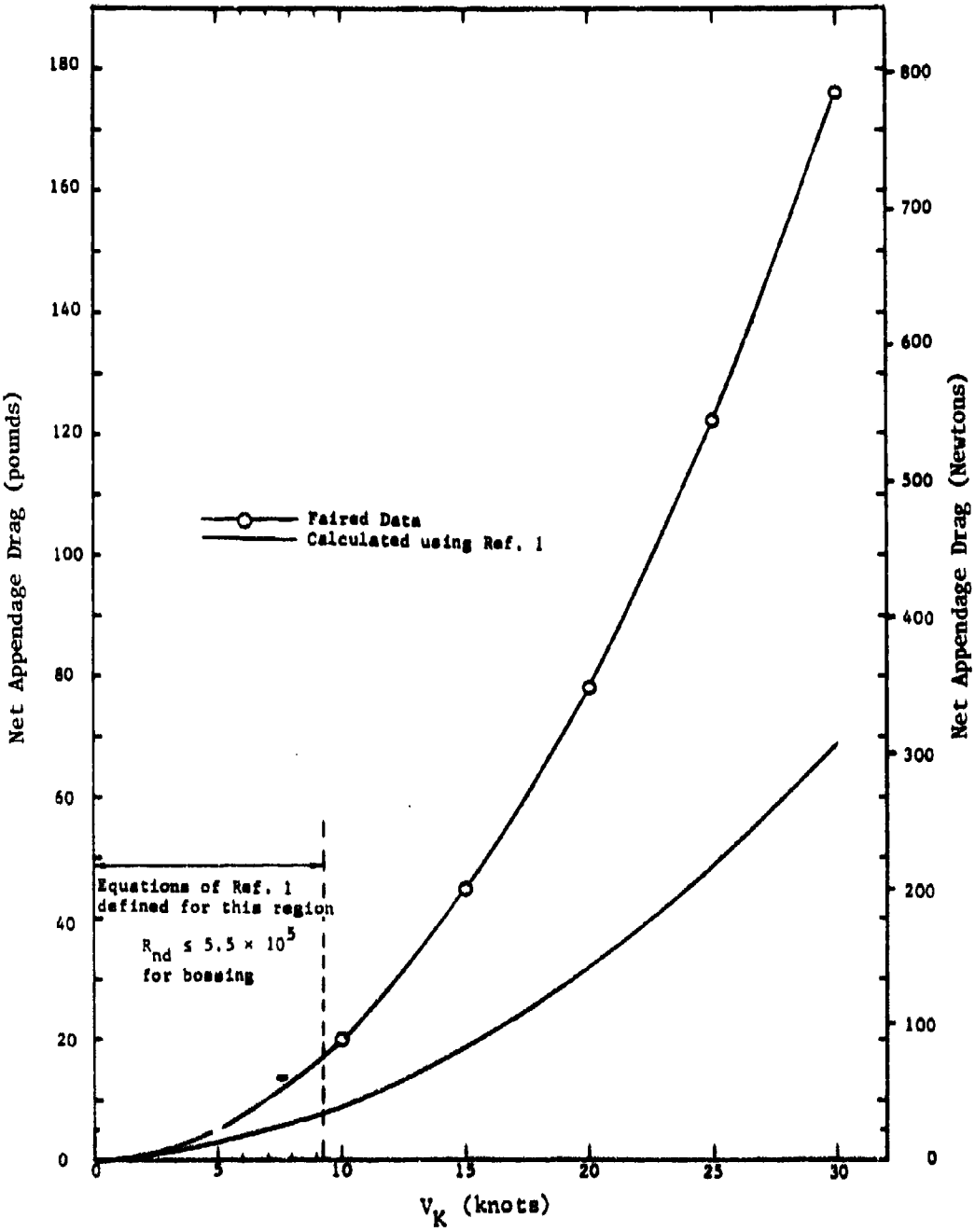

Figure 19 - Comparison Between Measured and Predicted Net Appendage Drag Plotted versus Speed, for the 10° Shaft, Single Strut Arrangement, Without Rudder

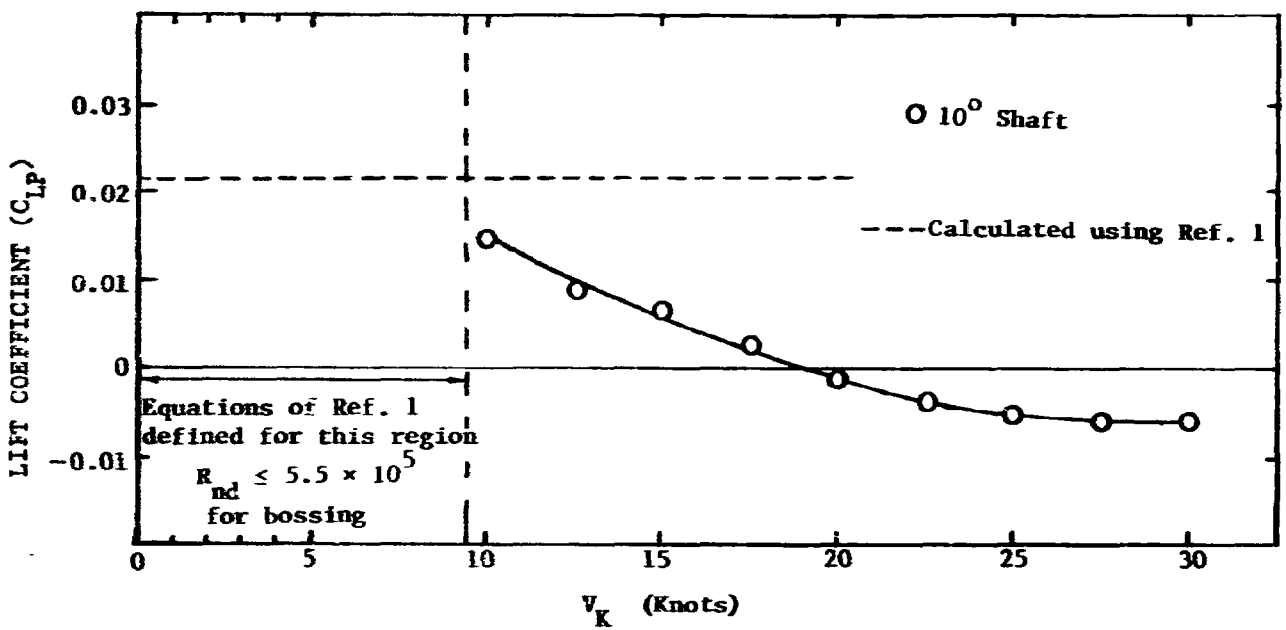

Figure 20 – Comparison Between Measured and Predicted Net Lift Coefficient Plotted versus Speed for the 10° Shaft, Single Strut Appendages, Without Rudder

TABLE 1

NET APPENDAGE DRAG CHARACTERISTICS: DIMENSIONAL FORCE SLOPES AND DRAG COEFFICIENTS

Shaft Angle/Configuration	Net Appendage Drag Force Slope $m_A = D_A V_K^{-2}$ $\frac{lbs}{Knot^2}$ ($\frac{Newtons}{Knot^2}$)	Appendage Drag Coefficient C_{DP}
7.5° with rudder	0.430 (1.91)	0.0714
7.5° without rudder	0.177 (0.787)	0.0294
10° with rudder	0.430 (1.91)	0.0714
10° without rudder	0.197 (0.876)	0.0327
15° with rudder	0.450 (2.00)	0.0747
15° without rudder	0.202 (0.898)	0.0336
10° V-struts with rudder	0.462 (2.05)	0.0767
10° V-struts w/o rudder	0.205 (0.912)	0.0341
Rudder only	0.333 (1.48)	0.0553 0.063 based on rudder planform area

TABLE 2

NET APPENDAGE DRAG FORCES, COMPARISON BETWEEN MEASURED AND PREDICTED VALUES FOR 10° SHAFT ANGLE, SINGLE STRUT ARRANGEMENT

V_K	Predicted Drag lbs (N)	Measured Drag lbs (N)	Measured Drag / Predicted Drag
10	8.7 (38.7)	19.7 (87.7)	2.3
15	18.6 (82.8)	44.2 (197)	2.4
20	31.9 (142)	78.6 (350)	2.5
25	48.6 (216)	123 (547)	2.5
30	68.5 (305)	177 (787)	2.6

DTNSRDC ISSUES THREE TYPES OF REPORTS

1. DTNSRDC REPORTS, A FORMAL SERIES, CONTAIN INFORMATION OF PERMANENT TECHNICAL VALUE. THEY CARRY A CONSECUTIVE NUMERICAL IDENTIFICATION REGARDLESS OF THEIR CLASSIFICATION OR THE ORIGINATING DEPARTMENT.

2. DEPARTMENTAL REPORTS, A SEMIFORMAL SERIES, CONTAIN INFORMATION OF A PRELIMINARY, TEMPORARY, OR PROPRIETARY NATURE OR OF LIMITED INTEREST OR SIGNIFICANCE. THEY CARRY A DEPARTMENTAL ALPHANUMERICAL IDENTIFICATION.

3. TECHNICAL MEMORANDA, AN INFORMAL SERIES, CONTAIN TECHNICAL DOCUMENTATION OF LIMITED USE AND INTEREST. THEY ARE PRIMARILY WORKING PAPERS INTENDED FOR INTERNAL USE. THEY CARRY AN IDENTIFYING NUMBER WHICH INDICATES THEIR TYPE AND THE NUMERICAL CODE OF THE ORIGINATING DEPARTMENT. ANY DISTRIBUTION OUTSIDE DTNSRDC MUST BE APPROVED BY THE HEAD OF THE ORIGINATING DEPARTMENT ON A CASE-BY-CASE BASIS.